Secrecy Performance Analysis on UAV Down-Link Broadcasting with a Full Duplex Receiver

Yuanjian Li and Mathini Sellathurai
Heriot-Watt University, Edinburgh, U.K.

A. Hamid Aghvami
King's College London, U.K.

***Abstract*—In this paper, physical layer security issue for a down-link wireless communication system is examined, composed of an unmanned aerial vehicle (UAV), a legitimate receiver and a passive eavesdropper. The destination is equipped with two antennas and applies the full-duplex (FD) Bob-based jamming (FD-BBJ) strategy to achieve secure transmission. Considering that practical air-to-ground (A2G) channels experience Nakagami-m fading and the FD legitimate receiver is affected by self-interference (SI), closed-form expressions of approximate ergodic achievable secrecy rate (EASR) with help of Gauss-Laguerre Quadrature (GLQ) and compact secrecy outage probability (SOP) expression are derived, respectively. To gain more insights, asymptotic secrecy performance is analysed in the case of extreme total system transmit power, via deriving closed-form expression for asymptotic EASR and compact expression for asymptotic SOP. Numerical results have verified the correctness of our theoretical analysis and proved that the FD-BBJ strategy applied in the UAV-aided wireless communication system can help achieve considerable secrecy performance gain.**

***Index Terms*—Physical layer security, full duplex, artificial noise, unmanned aerial vehicle, Gauss-Laguerre Quadrature.**

I. Introduction

Unmanned aerial vehicles (UAVs) have been widely used in many practical scenarios, e.g., surveillance, material transport and real estate photography. With high mobility, low cost and on-demand deployment, UAVs have also been increasingly applied in the field of wireless communications, for instance, mobile relaying, edge computing and coverage enhancement. Recently, UAV-aided wireless communications have been recognized as a promising way to solve challenging problems for the sixth generation (6G) wireless networks, such as super high-speed data transmission demands [1]. Compared to terrestrial communication networks that are based on fixed-location high-altitude platforms, UAV-aided wireless communication systems are able to establish short-distance links with line-of-sight (LoS) transmissions, resulting in better channel qualities among transceivers [2].

Unfortunately, due to the broadcasting nature of radio frequency (RF) medium, confidential information transmitted within UAV-aided wireless communication systems is vulnerable to being intercepted by malicious eavesdroppers. Therefore, transmission security has become an essential and important issue in the implementation and operation of UAV-aided networks. As a promising solution to realize secure transmissions, physical layer security (PLS) technique which directly exploits the randomness offered by wireless medium, has been receiving more and more research attention [3]–[5]. Different from conventional key-based cryptographic techniques applied to upper layers, PLS can safeguard secrecy wireless data transmissions without requiring secret keys or complex algorithms. As a widely used cooperative jamming (CJ) strategy in PLS regime, the full-duplex Bob-based jamming (FD-BBJ) scheme applied at the receiver can receive the intended signal and simultaneously broadcast the artificial noise (AN) to effectively reduce the probability of being eavesdropped [6]. Additionally, the FD-BBJ scheme is more reliable and simpler to be implemented compared to other CJ schemes using external helpers [7].

Although the PLS technique has been widely studied in the field of terrestrial wireless communications, PLS issue in the UAV-aided wireless transmission scenarios has not drawn much attention so far. Considering that UAVs have been widely used in military and civilian applications, it is essential to make a thorough inquiry for the PLS issue in UAV-aided wireless communication systems. Motivated by the above observations, we propose an FD-BBJ secure transmission scheme for the UAV-mounted wiretap channel, where a multi-antenna UAV transmits the confidential signal to the FD two-antenna legitimate receiver in the presence of a single-antenna passive eavesdropper. The main contributions of this paper are concluded as follows.

- With practical assumption on imperfect self-interference cancellation (SIC), closed-form cumulative distribution function (CDF) and probability density function (PDF) expressions of received signal-to-interference-and-noise ratios (SINRs) at the legitimate receiver and the eavesdropper are derived, respectively. Then, closed-form expression of the approximate ergodic achievable secrecy rate (EASR) and the compact expression of the secrecy outage probability (SOP) are calculated.
- To gain more insights, asymptotic secrecy performance of extreme total system transmit power is analysed, after deriving closed-form expression of the asymptotic EASR and compact expression of the asymptotic SOP.
- Numerical results are provided to validate correctness of the derived analytical formulas, showcase effectiveness of FD-BBJ solution for enhancing secrecy transmission of UAV-aided down-link broadcasting channels, and track impacts of various system parameters, e.g., transmit power, on the evaluated metrics.

II. System Model

A. UAV Down-link Broadcasting System

In a rural subregion, a UAV-enabled downlink wireless transmission scenario is considered within a three-dimensional (3D) Cartesian cylinder coordinate system where its radius is denoted as D, in which a UAV (Alice) transmits wireless messages to a legitimate receiver (Bob) in the presence of a passive eavesdropper (Eve). Besides, Bob is assumed to possess dual antennas, while Alice and Eve equip N_{A} antennas and a single antenna, respectively. Specifically, Bob is working in the FD mode with one antenna for AN emitting and the other for simultaneous information

reception. Due to UAV's high operational altitude and LoS-dominated air-to-ground (A2G) links, it becomes easier for ground-based malicious party to eavesdrop wireless signals emitted from UAVs, undoubtedly highlighting the importance of secrecy communications. To help achieve secure wireless transmissions, FD-BBJ strategy is adopted to allow Bob to generate AN for interfering with Eve's wiretap.

B. Channel Model

Wireless channels between Alice to Bob, Alice to Eve and Bob to Eve aredenoted as $\mathbf{h}_{\mathrm{AB}} = \left[h_{1,\mathrm{B}}, h_{2,\mathrm{B}}, \cdots, h_{N_{\mathrm{A}},\mathrm{B}}\right]$, $\mathbf{h}_{\mathrm{AE}} = \left[h_{1,\mathrm{E}}, h_{2,\mathrm{E}}, \cdots, h_{N_{\mathrm{A}},\mathrm{E}}\right]$ and h_{BE}, respectively, where $h_{i,\mathrm{B}}$ represents the channel coefficient between the i-th transmit antenna at Alice and Bob, and $h_{i,\mathrm{E}}$ is the channel coefficient between the i-th transmit antenna at Alice and Eve, with $i = 1, 2, \cdots, N_{\mathrm{A}}$. Due to the FD nature, there inevitably exists a self-interference (SI) link between Bob's dual antenna, which is denoted as h_{BB}. In this paper, a practical assumption of imperfect SI cancellation (SIC) is adopted, where the SI is considered to be partially suppressed. Note that the SIC technique, e.g., antenna isolation and analog/digital elimination, is of importance for unleashing the promised potentials of FD-aided transmissions because the presence of SI seriously constrains the received SINR at the FD transceiver. As we focus on a rural area, the A2G channels, i.e., $\mathbf{h}_{\mathrm{AB}}$ and $\mathbf{h}_{\mathrm{AE}}$, are assumed to be LoS-dominated. Rayleigh fading channel model is widely used to model RF channel owing to its analytical tractability, but it is not suitable in the A2G scenario due to the consideration of the LoS-dominated link. Therefore, all A2G channels are modelled as block Nakagami-m fading links, i.e., the channels remain static for one coherence interval and are subject to independent identically-distributed (i.i.d.) Nakagami-m fading with parameter m. Different from the A2G channel, the channels between the terrestrial devices, i.e., h_{BB} and h_{BE}, are subject to quasi-static i.i.d. Rayleigh fading due to the obstacles among terrestrial terminals. The squared means of all channel coefficients are set as $\mathbb{E}\{|h_{i\mathrm{B}}|^2\} = \Omega_{\mathrm{AB}}$, $\mathbb{E}\{|h_{i\mathrm{E}}|^2\} = \Omega_{\mathrm{AE}}$, $\mathbb{E}\{|h_{\mathrm{BE}}|^2\} = \Omega_{\mathrm{BE}}$ and $\mathbb{E}\{|h_{\mathrm{BB}}|^2\} = \Omega_{\mathrm{BB}}$, respectively. Moreover, the path loss model on the sub-6 GHz band is considered to characterize the large-scale fading for A2G wireless links, given by $\Psi_{\mathrm{A}j}(\mathrm{dB}) = 20\lg(d_{\mathrm{A}j}) + 20\lg(\varpi) - 147.55$, where $d_{\mathrm{A}j}$ denotes the Euclidean distance between Alice and $j \in (\mathrm{B}, \mathrm{E})$, and ϖ represents the carrier frequency. The distance and path loss exponent between Bob and Eve are denoted as d_{BE} and η_{BE}, respectively. Besides, $P_{\mathrm{A}} = \alpha P$ and $P_{\mathrm{B}} = (1-\alpha)P$ denote transmit power at Alice and Bob, with the total transmit power constraint $P_{\mathrm{A}} + P_{\mathrm{B}} = P$, where α is the power allocation factor.

C. System model

Due to UAV's scarcity of information processing capacity and on-board energy supply, in this paper, Alice is supposed to broadcast the intended information without any beamforming techniques. Then, the received signal at Bob and Eve can be formulated as

$$y_B = \sqrt{P_{\mathrm{A}} 10^{\frac{-\Psi_{\mathrm{AB}}}{10}}}\mathbf{h}_{\mathrm{AB}}\mathbf{s} + \sqrt{\rho P_{\mathrm{B}}}h_{\mathrm{BB}}v + n_{\mathrm{B}}, \quad (1)$$

$$y_E = \sqrt{P_{\mathrm{A}} 10^{\frac{-\Psi_{\mathrm{AE}}}{10}}}\mathbf{h}_{\mathrm{AE}}\mathbf{s} + \sqrt{P_{\mathrm{B}} d_{\mathrm{BE}}^{-\eta_{\mathrm{BE}}}}h_{\mathrm{BE}}v + n_{\mathrm{E}}, \quad (2)$$

where $\mathbf{s} \sim \mathcal{CN}(\mathbf{0}, \mathbf{I}/N_{\mathrm{A}})$ is the signal emitted from Alice, $\mathbf{I}$ denotes the $N_{\mathrm{A}} \times N_{\mathrm{A}}$ unit matrix and $v \sim \mathcal{CN}(0,1)$ is the AN signal used to interfere the eavesdropper. Moreover, $\rho \in [0,1]$ is a normalized coefficient which represents the degree of SIC, where $\rho = 1$ means that there is no SIC applied at Bob, while $\rho = 0$ signifies the perfect SIC and $\rho \in (0,1)$ denotes the imperfect SIC. Besides, n_{B} and n_{E} are the addictive white Gaussian noises (AWGNs) at Bob and Eve with zero mean and variances σ_{B}^2 and σ_{E}^2, respectively. From (1) and (2), the received SINRs at Bob and Eve can be calculated as

$$\gamma_{\mathrm{B}} = \frac{P_{\mathrm{A}} 10^{\frac{-\Psi_{\mathrm{AB}}}{10}} \|\mathbf{h}_{\mathrm{AB}}\|^2}{\rho N_{\mathrm{A}} P_{\mathrm{B}} |h_{\mathrm{BB}}|^2 + N_{\mathrm{A}}\sigma_{\mathrm{B}}^2}, \quad (3)$$

$$\gamma_{\mathrm{E}} = \frac{P_{\mathrm{A}} 10^{\frac{-\Psi_{\mathrm{AE}}}{10}} \|\mathbf{h}_{\mathrm{AE}}\|^2}{N_{\mathrm{A}} P_{\mathrm{B}} d_{\mathrm{BE}}^{-\eta_{\mathrm{BE}}} |h_{\mathrm{BE}}|^2 + N_{\mathrm{A}}\sigma_{\mathrm{E}}^2}. \quad (4)$$

III. Secrecy Performance Analysis

In the considered model, the secrecy capacity can be expressed as $C_{\mathrm{S}} = [C_{\mathrm{B}} - C_{\mathrm{E}}]^+$, where $[x]^+ \triangleq \max\{0, x\}$, and $C_{\mathrm{B}} = \log_2(1+\gamma_{\mathrm{B}})$ and $C_{\mathrm{E}} = \log_2(1+\gamma_{\mathrm{E}})$ are mutual information of the legitimate and eavesdropping channels, respectively. The ergodic secrecy capacity is defined as the rate below which any average secure communication rate is achievable and formulated under block fading channels as [8]

$$\begin{aligned}\mathbb{E}[C_{\mathrm{S}}] &= \int_0^\infty \int_0^\infty [C_{\mathrm{B}} - C_{\mathrm{E}}]^+ f(\gamma_{\mathrm{B}}) f(\gamma_{\mathrm{E}}) d\gamma_{\mathrm{B}} d\gamma_{\mathrm{E}} \\ &= \mathbb{E}\left[[C_{\mathrm{B}} - C_{\mathrm{E}}]^+\right]. \end{aligned} \quad (5)$$

However, the exact evaluation of (5) appears to be intractable for our considered system. Alternatively, we focus our analysis on a lower bound of (5), expressed as

$$\mathbb{E}[C_{\mathrm{S}}] \geq [\mathbb{E}[C_{\mathrm{B}}] - \mathbb{E}[C_{\mathrm{E}}]]^+ \triangleq \overline{C}_{\mathrm{S}}, \quad (6)$$

which is known as ergodic achievable secrecy rate (EASR).

Besides, the secrecy outage probability (SOP) is defined as the probability that the achievable secrecy rate is less than a given secrecy transmission rate R_{th}, below which secure transmission is not guaranteed. In our considered system, the SOP can be formulated as

$$P_{out}(R_{th}) = \Pr(C_S \leq R_{th}) = \Pr\left(\frac{1+\gamma_{\mathrm{B}}}{1+\gamma_{\mathrm{E}}} \leq 2^{R_{th}}\right). \quad (7)$$

A. Preliminaries

Since all the A2G channels are assumed to experience i.i.d. Nakagami-m fading, i.e., the envelope of $|h_{ij}|$ follows i.i.d. Nakagami-m distribution, and thus $|h_{ij}|^2$ must follow i.i.d. Gamma distribution with parameter m. Then, the PDF and the CDF of $|h_{ij}|^2$ can be given by

$$f_{|h_{ij}|^2}(x) = \frac{x^{m_j-1}}{\Gamma(m_j)}\left(\frac{m_j}{\Omega_{\mathrm{A}j}}\right)^{m_j} e^{-\frac{m_j}{\Omega_{\mathrm{A}j}}x}, \quad (8)$$

$$F_{|h_{ij}|^2}(x) = 1 - e^{-\frac{m_j}{\Omega_{\mathrm{A}j}}x}\sum_{p=0}^{m_j-1}\frac{1}{p!}\left(\frac{m_j}{\Omega_{\mathrm{A}j}}x\right)^p, \quad (9)$$

where $\mathbb{E}\left\{|h_{ij}|^2\right\} = \Omega_{\mathrm{A}j}$, $\Gamma(\cdot)$ is the Gamma function and $\Gamma(\cdot,\cdot)$ is the upper incomplete Gamma function. Note that m_j represents the Nakagami parameter of the channel between Alice and Bob or Eve.

Moreover, the CDF and PDF of $\|\mathbf{h}_{\mathrm{A}j}\|^2$ can be derived as

$$F_{\|\mathbf{h}_{\mathrm{A}j}\|^2}(x) = 1 - \frac{\Gamma\left(m_j N_{\mathrm{A}}, \frac{m_j}{\Omega_{\mathrm{A}j}}x\right)}{\Gamma(m_j N_{\mathrm{A}})}, \tag{10}$$

$$f_{\|\mathbf{h}_{\mathrm{A}j}\|^2}(x) = \frac{x^{m_j N_{\mathrm{A}}-1}}{\Gamma(m_j N_{\mathrm{A}})}\left(\frac{m_j}{\Omega_{\mathrm{A}j}}\right)^{m_j N_{\mathrm{A}}} e^{-\frac{m_j}{\Omega_{\mathrm{A}j}}x}. \tag{11}$$

All the terrestrial channels experience i.i.d. Rayleigh fading, thus $|h_{\mathrm{B}j}|^2$ follows i.i.d. Exponential distribution with parameter $1/\Omega_{\mathrm{B}j}$, where $\mathbb{E}\left\{|h_{\mathrm{B}j}|^2\right\} = \Omega_{\mathrm{B}j}$. Then, the PDF and CDF of $|h_{\mathrm{B}j}|^2$ are given by

$$f_{|h_{\mathrm{B}j}|^2}(x) = \frac{1}{\Omega_{\mathrm{B}j}} e^{-\frac{1}{\Omega_{\mathrm{B}j}}x}, \tag{12}$$

$$F_{|h_{\mathrm{B}j}|^2}(x) = 1 - e^{-\frac{1}{\Omega_{\mathrm{B}j}}x}. \tag{13}$$

B. The Statistics of γ_{B} and γ_{E}

Lemma 1: Closed-form expressions of CDF and PDF of γ_{B} are derived as (14) and (15), respectively.

Proof: The CDF of γ_{B} can be calculated as $P(\gamma_{\mathrm{B}} \leq x)$. After combining (10) and (13), closed-form CDF expression of γ_{B} is calculated as (14). The closed-form PDF expression of γ_{B} can be obtained by taking the derivative of (14) with respect to (w.r.t.) x. ■

Lemma 2: Closed-form expressions of CDF and PDF of γ_{E} are derived as (16) and (17), respectively.

Proof: Similar to proof of *Lemma 1*, thus omitted. ■

C. EASR Analysis

Theorem 1: The closed-form expression for the approximate ergodic achievable rate of the legitimate channel, i.e., $\mathbb{E}[C_{\mathrm{B}}]$, can be calculated as

$$\mathbb{E}[C_{\mathrm{B}}] \approx \frac{1}{\ln 2}\sum_{\varpi=1}^{\vartheta}\omega_{\varpi}\Phi(z_{\varpi}), \tag{18}$$

where z_{ϖ} $(\varpi = 0, 1, ..., \vartheta)$ is the ϖ-th root of the Laguerre polynomial $\mathcal{L}_{\vartheta}(z)$ and ω_{ϖ} which does not depend on $\Phi(z)$ is the ϖ-th weight given by

$$\omega_{\varpi} = \frac{z_{\varpi}}{\left[(\vartheta+1)\mathcal{L}_{\vartheta+1}(z_{\varpi})\right]^2}. \tag{19}$$

ϑ denotes the number of points used to approximate the integral. It is meaningful to note that both z_{ϖ} and ω_{ϖ} can be calculated efficiently using the algorithm provided in [9].

Proof: We can formulate $\mathbb{E}[C_{\mathrm{B}}]$ as

$$\begin{aligned}\mathbb{E}[C_{\mathrm{B}}] &= \frac{1}{\ln 2}\mathbb{E}[\ln(1+\gamma_{\mathrm{B}})] \\ &= \frac{1}{\ln 2}\int_0^{\infty}\frac{1-F_{\gamma_{\mathrm{B}}}(x)}{1+x}dx.\end{aligned} \tag{20}$$

Invoking (14) into (20), we can get the semi-closed-form expression of $\mathbb{E}[C_{\mathrm{B}}]$ as

$$\mathbb{E}[C_{\mathrm{B}}] = \frac{1}{\ln 2}\int_0^{+\infty} e^{-x}\Phi(x)\,dx. \tag{21}$$

where

$$\begin{aligned}\Phi(x) = &\sum_{u=0}^{m_{\mathrm{B}}N_{\mathrm{A}}-1}\sum_{v=0}^{u}\binom{u}{v}(N_{\mathrm{A}}m_{\mathrm{B}}x)^u\, v!\sigma_{\mathrm{B}}^{2(u-v)} \\ &\times \frac{P^{v-u}\left(\rho(1-\alpha)\Omega_{\mathrm{BB}}\right)^v}{\left(\rho(1-\alpha)N_{\mathrm{A}}m_{\mathrm{B}}\Omega_{\mathrm{BB}}x + \alpha 10^{\frac{-\Psi_{\mathrm{AB}}}{10}}\Omega_{\mathrm{AB}}\right)^{v+1}} \\ &\times \frac{e^x\left(\alpha 10^{\frac{-\Psi_{\mathrm{AB}}}{10}}\Omega_{\mathrm{AB}}\right)^{v+1-u}}{u!(1+x)}.\end{aligned} \tag{22}$$

The integral in (21) can not be derived to a closed-form. As such, we resort to adopt the Gauss-Laguerre Quadrature (GLQ) method [10] to approach the integral with finite summation. Then, (18) can be obtained. ■

Theorem 2: Closed-form expression of the approximate ergodic achievable rate of the eavesdropping channel, i.e., $\mathbb{E}[C_{\mathrm{E}}]$, can be derived as

$$\mathbb{E}[C_{\mathrm{E}}] \approx \frac{1}{\ln 2}\sum_{\varpi=1}^{\vartheta}\omega_{\varpi}\mathcal{H}(z_{\varpi}), \tag{23}$$

where

$$\begin{aligned}\mathcal{H}(x) = &\sum_{p=0}^{m_E N_{\mathrm{A}}-1}\sum_{q=0}^{p}\binom{p}{q}(N_{\mathrm{A}}m_{\mathrm{E}}x)^p\, q!\sigma_{\mathrm{E}}^{2(p-q)} \\ &\times \frac{P^{q-p}\left((1-\alpha)d_{\mathrm{BE}}^{-\eta_{\mathrm{BE}}}\Omega_{\mathrm{BE}}\right)^q}{\left((1-\alpha)N_{\mathrm{A}}m_{\mathrm{E}}d_{\mathrm{BE}}^{-\eta_{\mathrm{BE}}}\Omega_{\mathrm{BE}}x + \alpha 10^{\frac{-\Psi_{\mathrm{AE}}}{10}}\Omega_{\mathrm{AE}}\right)^{q+1}} \\ &\times \frac{e^x\left(\alpha 10^{\frac{-\Psi_{\mathrm{AE}}}{10}}\Omega_{\mathrm{AE}}\right)^{q+1-p}}{p!(1+x)}.\end{aligned} \tag{24}$$

Proof: Similar to proof of *Theorem 1*, thus omitted. ■

From *Theorem 1*, *Theorem 2* and (6), Closed-form expression of the approximate EASR can be formulated as

$$\overline{C}_{\mathrm{S}} \approx \frac{1}{\ln 2}\left[\sum_{\varpi=1}^{\vartheta}\omega_{\varpi}\Phi(z_{\varpi}) - \sum_{\varpi=1}^{\vartheta}\omega_{\varpi}\mathcal{H}(z_{\varpi})\right]^+. \tag{25}$$

D. SOP Analysis

Theorem 3: The compact SOP expression of the considered model is given by (26).

Proof: Invoking (7), (14) and (17) and after some mathematical manipulations, (26) can be derived, where step (a) stands due to the binomial expansion, i.e., $\left[2^{R_{th}}(1+x)-1\right]^u = \sum_{\varepsilon=0}^{u}\left(2^{R_{th}}x\right)^{\varepsilon}\left(2^{R_{th}}-1\right)^{u-\varepsilon}$. ■

IV. Asymptotic Secrecy Performance Analysis

Closed-form expressions of approximate EASR and the compact SOP expression have been calculated in the last section. To gain simple yet meaningful conclusions and analyse the secure performance of the considered system more effectively, in this section, we will provide analysis for EASR and SOP in the asymptotic case where the total transmit power of the system tends to infinity, i.e., $P \to +\infty$.

A. Asymptotic EASR Analysis

Lemma 3: In the case of $P \to +\infty$, closed-form CDF and PDF expressions of γ_j are given by (27), (28), (29) and (30), respectively.

Proof: If $P \to +\infty$, (3) and (4) are rewritten as

$$\gamma_{\mathrm{B}}^{P\to+\infty} = \frac{\alpha 10^{\frac{-\Psi_{\mathrm{AB}}}{10}}\|\mathbf{h}_{\mathrm{AB}}\|^2}{\rho(1-\alpha)N_{\mathrm{A}}|h_{\mathrm{BB}}|^2}, \tag{31}$$

$$F_{\gamma_{\mathrm{B}}}(x)=1-\sum_{u=0}^{m_{\mathrm{B}}N_{\mathrm{A}}-1}\sum_{v=0}^{u}\binom{u}{v}\left(N_{\mathrm{A}}m_{\mathrm{B}}x\right)^{u}v!\sigma_{\mathrm{B}}^{2(u-v)}\frac{P^{v-u}\left(\alpha 10^{\frac{-\Psi_{\mathrm{AB}}}{10}}\Omega_{\mathrm{AB}}\right)^{v+1-u}\left(\rho\left(1-\alpha\right)\Omega_{\mathrm{BB}}\right)^{v}}{u!\left(\rho\left(1-\alpha\right)N_{\mathrm{A}}m_{\mathrm{B}}\Omega_{\mathrm{BB}}x+\alpha 10^{\frac{-\Psi_{\mathrm{AB}}}{10}}\Omega_{\mathrm{AB}}\right)^{v+1}} \tag{14}$$

$$f_{\gamma_{\mathrm{B}}}(x)=\sum_{u=0}^{m_{\mathrm{B}}N_{\mathrm{A}}-1}\sum_{v=0}^{u}\binom{u}{v}v!\left(\alpha 10^{\frac{-\Psi_{\mathrm{AB}}}{10}}\Omega_{\mathrm{AB}}\right)^{v+1-u}P^{v-u}\frac{\sigma_{\mathrm{B}}^{2(u-v)}\left(\rho\left(1-\alpha\right)\Omega_{\mathrm{BB}}\right)^{v}\left(N_{\mathrm{A}}m_{\mathrm{B}}\right)^{u}x^{u-1}}{u!\left(\rho\left(1-\alpha\right)N_{\mathrm{A}}m_{\mathrm{B}}\Omega_{\mathrm{BB}}x+\alpha 10^{\frac{-\Psi_{\mathrm{AB}}}{10}}\Omega_{\mathrm{AB}}\right)^{v+2}}$$
$$\times\left[\alpha 10^{\frac{-\Psi_{\mathrm{AB}}}{10}}\Omega_{\mathrm{AB}}u+\rho\left(1-\alpha\right)N_{\mathrm{A}}m_{\mathrm{B}}\Omega_{\mathrm{BB}}\left(u-v-1\right)x\right] \tag{15}$$

$$F_{\gamma_{\mathrm{E}}}(x)=1-\sum_{p=0}^{m_{E}N_{\mathrm{A}}-1}\sum_{q=0}^{p}\binom{p}{q}\left(N_{\mathrm{A}}m_{\mathrm{E}}x\right)^{p}q!\sigma_{\mathrm{E}}^{2(p-q)}\frac{P^{q-p}\left(\alpha 10^{\frac{-\Psi_{\mathrm{AE}}}{10}}\Omega_{\mathrm{AE}}\right)^{q+1-p}\left(\left(1-\alpha\right)d_{\mathrm{BE}}^{-\eta_{\mathrm{BE}}}\Omega_{\mathrm{BE}}\right)^{q}}{p!\left(\left(1-\alpha\right)N_{\mathrm{A}}m_{\mathrm{E}}d_{\mathrm{BE}}^{-\eta_{\mathrm{BE}}}\Omega_{\mathrm{BE}}x+\alpha 10^{\frac{-\Psi_{\mathrm{AE}}}{10}}\Omega_{\mathrm{AE}}\right)^{q+1}} \tag{16}$$

$$f_{\gamma_{\mathrm{E}}}(x)=\sum_{p=0}^{m_{\mathrm{E}}N_{\mathrm{A}}-1}\sum_{q=0}^{p}\binom{p}{q}q!\left(\alpha 10^{\frac{-\Psi_{\mathrm{AE}}}{10}}\Omega_{\mathrm{AE}}\right)^{q+1-p}\frac{P^{q-p}\sigma_{\mathrm{E}}^{2(p-q)}\left(\left(1-\alpha\right)d_{\mathrm{BE}}^{-\eta_{\mathrm{BE}}}\Omega_{\mathrm{BE}}\right)^{q}\left(N_{\mathrm{A}}m_{\mathrm{E}}\right)^{p}x^{p-1}}{p!\left(N_{\mathrm{A}}m_{\mathrm{B}}\left(1-\alpha\right)d_{\mathrm{BE}}^{-\eta_{\mathrm{BE}}}\Omega_{\mathrm{BE}}x+\alpha 10^{\frac{-\Psi_{\mathrm{AE}}}{10}}\Omega_{\mathrm{AE}}\right)^{q+2}}$$
$$\times\left[\alpha 10^{\frac{-\Psi_{\mathrm{AE}}}{10}}\Omega_{\mathrm{AE}}p+\left(1-\alpha\right)N_{\mathrm{A}}m_{\mathrm{E}}d_{\mathrm{BE}}^{-\eta_{\mathrm{BE}}}\Omega_{\mathrm{BE}}\left(p-q-1\right)x\right] \tag{17}$$

$$P_{out}=1-\sum_{u=0}^{m_{\mathrm{B}}N_{\mathrm{A}}-1}\sum_{v=0}^{u}\sum_{p=0}^{m_{E}N_{\mathrm{A}}-1}\sum_{q=0}^{p}\binom{u}{v}\binom{p}{q}\frac{v!q!\sigma_{\mathrm{B}}^{2(u-v)}\sigma_{\mathrm{E}}^{2(p-q)}P^{v+q-u-p}N_{\mathrm{A}}^{u+p}m_{\mathrm{B}}^{u}m_{\mathrm{E}}^{p}\alpha^{v+q+2-u-p}\left(1-\alpha\right)^{v+q}}{u!p!}$$
$$\times\left(10^{\frac{-\Psi_{\mathrm{AB}}}{10}}\Omega_{\mathrm{AB}}\right)^{v+1-u}\left(\rho\Omega_{\mathrm{BB}}\right)^{v}\left(10^{\frac{-\Psi_{\mathrm{AE}}}{10}}\Omega_{\mathrm{AE}}\right)^{q+1-p}\left(d_{\mathrm{BE}}^{-\eta_{\mathrm{BE}}}\Omega_{\mathrm{BE}}\right)^{q}$$
$$\times\int_{0}^{+\infty}\frac{\left[2^{R_{th}}\left(1+x\right)-1\right]^{u}}{\left(\rho\left(1-\alpha\right)N_{\mathrm{A}}m_{\mathrm{B}}\Omega_{\mathrm{BB}}\left(2^{R_{th}}\left(1+x\right)-1\right)+\alpha 10^{\frac{-\Psi_{\mathrm{AB}}}{10}}\Omega_{\mathrm{AB}}\right)^{v+1}}$$
$$\times\frac{\left[\alpha 10^{\frac{-\Psi_{\mathrm{AE}}}{10}}\Omega_{\mathrm{AE}}p+\left(1-\alpha\right)N_{\mathrm{A}}m_{\mathrm{E}}d_{\mathrm{BE}}^{-\eta_{\mathrm{BE}}}\Omega_{\mathrm{BE}}\left(p-q-1\right)x\right]x^{p-1}}{\left(N_{\mathrm{A}}m_{\mathrm{E}}\left(1-\alpha\right)d_{\mathrm{BE}}^{-\eta_{\mathrm{BE}}}\Omega_{\mathrm{BE}}x+\alpha 10^{\frac{-\Psi_{\mathrm{AE}}}{10}}\Omega_{\mathrm{AE}}\right)^{q+2}}dx$$
$$\overset{a}{=}1-\sum_{u=0}^{m_{\mathrm{B}}N_{\mathrm{A}}-1}\sum_{v=0}^{u}\sum_{p=0}^{m_{E}N_{\mathrm{A}}-1}\sum_{q=0}^{p}\sum_{\varepsilon=0}^{u}\binom{u}{v}\binom{p}{q}\frac{\left(10^{\frac{-\Psi_{\mathrm{AB}}}{10}}\Omega_{\mathrm{AB}}\right)^{v+1-u}\left(\rho\Omega_{\mathrm{BB}}\right)^{v}\left(10^{\frac{-\Psi_{\mathrm{AE}}}{10}}\Omega_{\mathrm{AE}}\right)^{q+1-p}\left(d_{\mathrm{BE}}^{-\eta_{\mathrm{BE}}}\Omega_{\mathrm{BE}}\right)^{q}}{u!p!}$$
$$\times 2^{R_{th}\varepsilon}\left(2^{R_{th}}-1\right)^{u-\varepsilon}v!q!\sigma_{\mathrm{B}}^{2(u-v)}\sigma_{\mathrm{E}}^{2(p-q)}P^{v+q-u-p}N_{\mathrm{A}}^{u+p}m_{\mathrm{B}}^{u}m_{\mathrm{E}}^{p}\alpha^{v+q+2-u-p}\left(1-\alpha\right)^{v+q}$$
$$\times\int_{0}^{+\infty}\frac{\left[\alpha 10^{\frac{-\Psi_{\mathrm{AE}}}{10}}\Omega_{\mathrm{AE}}p+\left(1-\alpha\right)N_{\mathrm{A}}m_{\mathrm{E}}d_{\mathrm{BE}}^{-\eta_{\mathrm{BE}}}\Omega_{\mathrm{BE}}\left(p-q-1\right)x\right]x^{p+\varepsilon-1}}{\left(\rho\left(1-\alpha\right)N_{\mathrm{A}}m_{\mathrm{B}}\Omega_{\mathrm{BB}}\left(2^{R_{th}}\left(1+x\right)-1\right)+\alpha 10^{\frac{-\Psi_{\mathrm{AB}}}{10}}\Omega_{\mathrm{AB}}\right)^{v+1}}$$
$$\times\frac{1}{\left(N_{\mathrm{A}}m_{\mathrm{E}}\left(1-\alpha\right)d_{\mathrm{BE}}^{-\eta_{\mathrm{BE}}}\Omega_{\mathrm{BE}}x+\alpha 10^{\frac{-\Psi_{\mathrm{AE}}}{10}}\Omega_{\mathrm{AE}}\right)^{q+2}}dx \tag{26}$$

$$F_{\gamma_{\mathrm{B}}^{P\to+\infty}}(x)=1-\sum_{u=0}^{m_{\mathrm{B}}N_{\mathrm{A}}-1}\frac{\alpha 10^{\frac{-\Psi_{\mathrm{AB}}}{10}}\Omega_{\mathrm{AB}}\left[\rho\left(1-\alpha\right)N_{\mathrm{A}}m_{\mathrm{B}}\Omega_{\mathrm{BB}}x\right]^{u}}{\left[\rho\left(1-\alpha\right)N_{\mathrm{A}}m_{\mathrm{B}}\Omega_{\mathrm{BB}}x+\alpha 10^{\frac{-\Psi_{\mathrm{AB}}}{10}}\Omega_{\mathrm{AB}}\right]^{u+1}} \tag{27}$$

$$f_{\gamma_{\mathrm{B}}^{P\to+\infty}}(x)=\sum_{u=0}^{m_{\mathrm{B}}N_{\mathrm{A}}-1}\frac{\alpha 10^{\frac{-\Psi_{\mathrm{AB}}}{10}}\Omega_{\mathrm{AB}}\left[\rho(1-\alpha)N_{\mathrm{A}}m_{\mathrm{B}}\Omega_{\mathrm{BB}}\right]^{u}x^{u-1}\left(\alpha u 10^{\frac{-\Psi_{\mathrm{AB}}}{10}}\Omega_{\mathrm{AB}}-\rho(1-\alpha)N_{\mathrm{A}}m_{\mathrm{B}}\Omega_{\mathrm{BB}}x\right)}{\left[\rho(1-\alpha)N_{\mathrm{A}}m_{\mathrm{B}}\Omega_{\mathrm{BB}}x+\alpha 10^{\frac{-\Psi_{\mathrm{AB}}}{10}}\Omega_{\mathrm{AB}}\right]^{u+2}} \tag{28}$$

$$F_{\gamma_{\mathrm{E}}^{P\to+\infty}}(x)=1-\sum_{p=0}^{m_{\mathrm{E}}N_{\mathrm{A}}-1}\frac{\alpha 10^{\frac{-\Psi_{\mathrm{AE}}}{10}}\Omega_{\mathrm{AE}}\left[(1-\alpha)N_{\mathrm{A}}d_{\mathrm{BE}}^{-\eta_{\mathrm{BE}}}m_{\mathrm{E}}\Omega_{\mathrm{BE}}x\right]^{p}}{\left[(1-\alpha)N_{\mathrm{A}}d_{\mathrm{BE}}^{-\eta_{\mathrm{BE}}}m_{\mathrm{E}}\Omega_{\mathrm{BE}}x+\alpha 10^{\frac{-\Psi_{\mathrm{AE}}}{10}}\Omega_{\mathrm{AE}}\right]^{p+1}} \tag{29}$$

$$f_{\gamma_{\mathrm{E}}^{P\to+\infty}}(x)=\sum_{p=0}^{m_{\mathrm{E}}N_{\mathrm{A}}-1}\frac{\alpha 10^{\frac{-\Psi_{\mathrm{AE}}}{10}}\Omega_{\mathrm{AE}}\left[(1-\alpha)N_{\mathrm{A}}d_{\mathrm{BE}}^{-\eta_{\mathrm{BE}}}m_{\mathrm{E}}\Omega_{\mathrm{BE}}\right]^{p}x^{p-1}\left(\alpha p 10^{\frac{-\Psi_{\mathrm{AE}}}{10}}\Omega_{\mathrm{AE}}-(1-\alpha)N_{\mathrm{A}}d_{\mathrm{BE}}^{-\eta_{\mathrm{BE}}}m_{\mathrm{E}}\Omega_{\mathrm{BE}}x\right)}{\left[(1-\alpha)N_{\mathrm{A}}d_{\mathrm{BE}}^{-\eta_{\mathrm{BE}}}m_{\mathrm{E}}\Omega_{\mathrm{BE}}x+\alpha 10^{\frac{-\Psi_{\mathrm{AE}}}{10}}\Omega_{\mathrm{AE}}\right]^{p+2}} \tag{30}$$

$$\gamma_{\mathrm{E}}^{P\to+\infty}=\frac{\alpha 10^{\frac{-\Psi_{\mathrm{AE}}}{10}}\|\mathbf{h}_{\mathrm{AE}}\|^{2}}{(1-\alpha)N_{\mathrm{A}}d_{\mathrm{BE}}^{-\eta_{\mathrm{BE}}}|h_{\mathrm{BE}}|^{2}}. \tag{32}$$

Combining (10), (12), (31) and (32), we can obtain (27) and (29). Note that (28) and (30) can be calculated from taking the derivatives of (27) and (29) w.r.t. x, respectively. ■

Theorem 4: Closed-form expression of asymptotic EASR in the case of $P\to+\infty$ can be derived as (33), where $\mathrm{B}(\cdot,\cdot,\cdot)$ represents the incomplete Beta function and $\csc(\cdot)$ denotes the cosection function.

Proof: Similar to the derivation of (25), invoking (27) and (29), (33) can be obtained. ■

B. Asymptotic SOP Analysis

Theorem 5: The compact expression of SOP when $P\to+\infty$ can be derived as (34).

Proof: The asymptotic SOP can be derived as $\Pr\left(\frac{1+\gamma_{\mathrm{B}}^{P\to+\infty}}{1+\gamma_{\mathrm{E}}^{P\to+\infty}}\le 2^{R_{th}}\right)$ in the case of $P\to+\infty$. Combining (27) and (30), (34) can be derived. ■

V. Numerical Results

In this section, we will show the numerical results to validate EASR and SOP analyses through Monte Carlo simulation method and then explore the impact of parameters on the considered metrics. EASR and SOP curves are generated from the analytical results of (25) and (26), while the asymptotic curves are plotted as per (33) and (34), respectively. The Monte Carlo simulation points are calculated by taking average over 10^6 random channel realizations. Without loss of generality, we assume unit variance for all involved channel coefficients and AWGNs' variances are given by $\sigma_{\mathrm{B}}^2=\sigma_{\mathrm{E}}^2=-60$dBm, while the carrier frequency is fixed at $\varpi=2$GHz. Path loss exponent for terrestrial transmission is adopted as $\eta_{\mathrm{BE}}=3$, while Nakagami parameters are considered as $m_{\mathrm{B}}=m_{\mathrm{E}}=2$. The amount of GLQ points used to approximate the EASR is set as $\vartheta=24$.

In Fig. 1, the approximate and asymptotic EASR curves versus P for various ρ are depicted, with $\alpha=0.5$, $N_{\mathrm{A}}=2$, $d_{\mathrm{BE}}=5$m, $d_{\mathrm{AB}}=30$m and $d_{\mathrm{AE}}=30$m. We can see that approximate EASR curves match well with the simulation results, which proves the feasibility of GLQ method. With the increase of ρ, EASR performance decreases significantly, revealing the necessity and importance of SIC. Besides, with the increase of P, EASR curves approach the asymptotic EASR lines, which validates the correctness of *Theorem 4*. We can also see that there is a performance cap for the considered system in the case of $P\to+\infty$, while the ceiling is irrelevant to P. Thus, to enhance the system's secrecy performance, one should avoid increasing the total transmit power blindly. Most importantly, even with imperfect SIC, the considered FD-BBJ strategy can help achieve significant EASR gain compared to that without (w/o) FD-BBJ, highlighting that FD-BBJ scheme is able to help enhance secrecy transmission performance for UAV-aided down-link broadcasting channels.

Fig. 2 shows SOP performance versus P for various d_{AB}, with $\rho=0.001$, $\alpha=0.5$, $N_{\mathrm{A}}=2$, $d_{\mathrm{BE}}=5$m, $d_{\mathrm{AE}}=30$m and $R_{th}=1$bps/Hz. It is straightforward to observe that analytical curves tightly match the simulation points and approach the asymptotic lines with the increase of P, verifying the correctness of *Theorem 3* and *Theorem 5*, respectively. We then observe that the SOP decreases with the increase of P. However, there exists a floor which is irrelevant to P on the SOP performance with the increase of P. Besides, a shorter distance between Alice and Bob is preferred, which can help the legitimate party suffer from less degree of SOP.

VI. Conclusions

In this paper, we examined an FD-BBJ strategy for safeguarding UAV-aided wireless down-link transmissions. To analyse the secrecy performance, with practical consideration of imperfect SIC at the legitimate receiver, we derived closed-form approximate EASR expression by adopting Gauss-Laguerre Quadrature (GLQ), and compact SOP expression, respectively. To gain more insights, we developed asymptotic secrecy performance analysis and derived closed-form asymptotic EASR expression and the compact asymptotic SOP expression, in the case of extreme total transmit power, i.e., $P\to+\infty$. Numerical results verified the correctness of our theoretical analysis and proved that the FD-BBJ strategy applied in the UAV-aided wireless communication system can help achieve considerable secrecy performance gain.

References

[1] G. Geraci, A. Garcia-Rodriguez, M. M. Azari, A. Lozano, M. Mezzavilla, S. Chatzinotas, Y. Chen, S. Rangan, and M. Di Renzo,

$$\overline{C}_{\mathrm{S}}^{P\to+\infty} = -\sum_{u=0}^{m_{\mathrm{B}}N_{\mathrm{A}}-1} \frac{\alpha 10^{\frac{-\Psi_{\mathrm{AB}}}{10}}\Omega_{\mathrm{AB}}\left[\rho\left(1-\alpha\right)N_{\mathrm{A}}m_{\mathrm{B}}\Omega_{\mathrm{BB}}\right]^{u}\left[\mathrm{B}\left(\frac{\rho(1-\alpha)N_{\mathrm{A}}m_{\mathrm{B}}\Omega_{\mathrm{BB}}}{\alpha 10^{\frac{-\Psi_{\mathrm{AB}}}{10}}\Omega_{\mathrm{AB}}},-u,u+1\right)+\pi\csc\left(u\pi\right)\right]}{\left(\alpha 10^{\frac{-\Psi_{\mathrm{AB}}}{10}}\Omega_{\mathrm{AB}}-\rho\left(1-\alpha\right)N_{\mathrm{A}}m_{\mathrm{B}}\Omega_{\mathrm{BB}}\right)^{u+1}}$$
$$+\sum_{p=0}^{m_{\mathrm{E}}N_{\mathrm{A}}-1} \frac{\alpha 10^{\frac{-\Psi_{\mathrm{AE}}}{10}}\Omega_{\mathrm{AE}}\left[\left(1-\alpha\right)N_{\mathrm{A}}d_{\mathrm{BE}}^{-\eta_{\mathrm{BE}}}m_{\mathrm{E}}\Omega_{\mathrm{BE}}\right]^{p}\left[\mathrm{B}\left(\frac{(1-\alpha)N_{\mathrm{A}}d_{\mathrm{BE}}^{-\eta_{\mathrm{BE}}}m_{\mathrm{E}}\Omega_{\mathrm{BE}}}{\alpha 10^{\frac{-\Psi_{\mathrm{AE}}}{10}}\Omega_{\mathrm{AE}}},-p,p+1\right)+\pi\csc\left(p\pi\right)\right]}{\left(\alpha 10^{\frac{-\Psi_{\mathrm{AE}}}{10}}\Omega_{\mathrm{AE}}-\left(1-\alpha\right)N_{\mathrm{A}}d_{\mathrm{BE}}^{-\eta_{\mathrm{BE}}}m_{\mathrm{E}}\Omega_{\mathrm{BE}}\right)^{p+1}} \tag{33}$$

$$P_{out}^{P\to+\infty} = 1-\sum_{u=0}^{m_{\mathrm{B}}N_{\mathrm{A}}-1}\sum_{p=0}^{m_{E}N_{\mathrm{A}}-1}\sum_{q=0}^{u}\binom{u}{q}\frac{\alpha 10^{\frac{-\Psi_{\mathrm{AB}}}{10}}\Omega_{\mathrm{AB}}\left[\rho\left(1-\alpha\right)N_{\mathrm{A}}m_{\mathrm{B}}\Omega_{\mathrm{BB}}\right]^{u}2^{qR_{th}}\left(2^{R_{th}}-1\right)^{u-q}}{u!p!}$$
$$\times\,\alpha 10^{\frac{-\Psi_{\mathrm{AE}}}{10}}\Omega_{\mathrm{AE}}\left[\left(1-\alpha\right)N_{\mathrm{A}}d_{\mathrm{BE}}^{-\eta_{\mathrm{BE}}}m_{\mathrm{E}}\Omega_{\mathrm{BE}}\right]^{p}$$
$$\times\int_{0}^{+\infty}\frac{\left[\alpha p 10^{\frac{-\Psi_{\mathrm{AE}}}{10}}\Omega_{\mathrm{AE}}-\left(1-\alpha\right)N_{\mathrm{A}}d_{\mathrm{BE}}^{-\eta_{\mathrm{BE}}}m_{\mathrm{E}}\Omega_{\mathrm{BE}}x\right]x^{p+q-1}}{\left(\rho\left(1-\alpha\right)N_{\mathrm{A}}m_{\mathrm{B}}\Omega_{\mathrm{BB}}\left(2^{R_{th}}\left(1+x\right)-1\right)+\alpha 10^{\frac{-\Psi_{\mathrm{AB}}}{10}}\Omega_{\mathrm{AB}}\right)^{u+1}}$$
$$\times\frac{1}{\left(N_{\mathrm{A}}m_{\mathrm{E}}\left(1-\alpha\right)d_{\mathrm{BE}}^{-\eta_{\mathrm{BE}}}\Omega_{\mathrm{BE}}x+\alpha 10^{\frac{-\Psi_{\mathrm{AE}}}{10}}\Omega_{\mathrm{AE}}\right)^{p+2}}dx \tag{34}$$

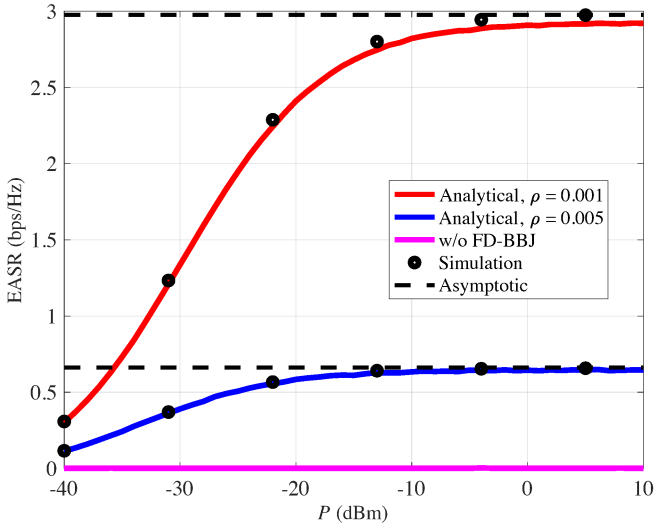

Fig. 1. EASR versus P for various ρ.

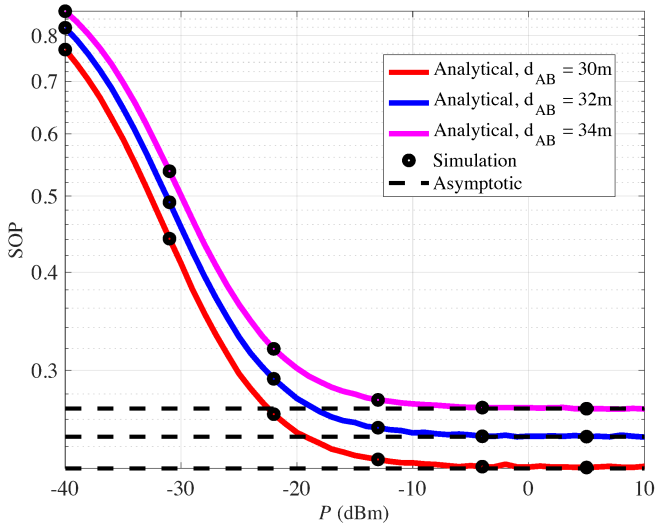

Fig. 2. SOP versus P for different d_{AB}.

"What will the future of UAV cellular communications be? a flight from 5G to 6G," *IEEE Commun. Surv. Tutor.*, vol. 24, no. 3, pp. 1304–1335, 2022.

[2] M. Mozaffari, W. Saad, M. Bennis, and M. Debbah, "Mobile unmanned aerial vehicles (UAVs) for energy-efficient internet of things communications," *IEEE Trans. Wireless Commun.*, vol. 16, no. 11, pp. 7574–7589, Sep. 2017.

[3] A. Kumar, S. Majhi, and H.-C. Wu, "Physical-layer security of underlay MIMO-D2D communications by null steering method over Nakagami-m and Norton fading channels," *IEEE Trans. Wireless Commun.*, vol. 21, no. 11, pp. 9700–9711, 2022.

[4] J. Qin and J. Liu, "Multi-access edge offloading based on physical layer security in C-V2X system," *IEEE Trans. Veh. Technol.*, vol. 71, no. 7, pp. 6912–6923, 2022.

[5] L. Sun and X. Tian, "Physical layer security in multi-antenna cellular systems: Joint optimization of feedback rate and power allocation," *IEEE Trans. Wireless Commun.*, vol. 21, no. 9, pp. 7165–7180, 2022.

[6] G. Zheng, I. Krikidis, J. Li, A. P. Petropulu, and B. Ottersten, "Improving physical layer secrecy using full-duplex jamming receivers," *IEEE Trans. Signal Process.*, vol. 61, no. 20, pp. 4962–4974, 2013.

[7] Y. Li, R. Zhao, L. Fan, and A. Liu, "Antenna mode switching for full-duplex destination-based jamming secure transmission," *IEEE Access*, vol. 6, no. 3, pp. 9442 – 9453, Mar. 2018.

[8] M. Bloch, J. Barros, M. R. Rodrigues, and S. W. McLaughlin, "Wireless information-theoretic security," *IEEE Trans. Inf. Theory*, vol. 54, no. 6, pp. 2515–2534, Jun. 2008.

[9] G. W. Recktenwald, *Numerical Methods with MATLAB: Implementation and Application*, 2000.

[10] S. Yan, N. Yang, R. Malaney, and J. Yuan, "Antenna switching for security enhancement in full-duplex wiretap channels," in *Proc. IEEE GLOBECOM Workshops*, Dec. 2014.